Engineering Nanoscale Surface Features to Sustain Microparticle Rolling in Flow

Surachate Kalasin and Maria M. Santore*

Department of Polymer Science and Engineering, University of Massachusetts Amherst, 120 Governors Drive, Amherst, Massachusetts 01003, United States

ABSTRACT Nanoscopic features of channel walls are often engineered to facilitate microfluidic transport, for instance when surface charge enables electro-osmosis or when grooves drive mixing. The dynamic or rolling adhesion of flowing microparticles on a channel wall holds potential to accomplish particle sorting or to selectively transfer reactive species or signals between the wall and flowing particles. Inspired by cell rolling under the direction of adhesion molecules called selectins, we present an engineered platform in which the rolling of flowing microparticles is sustained through the incorporation of entirely synthetic, discrete, nanoscale, attractive features into the nonadhesive (electrostatically repulsive) surface of a flow channel. Focusing on one example or type of nanoscale feature and probing the impact of broad systematic variations in surface feature loading and processing parameters, this study demonstrates how relatively flat, weakly adhesive nanoscale features, positioned with average spacings on the order of tens of nanometers, can produce sustained microparticle rolling. We further demonstrate how the rolling velocity and travel distance depend on flow and surface design. We identify classes of related surfaces that fail to support rolling and present a state space that identifies combinations of surface and processing variables corresponding to transitions between rolling, free particle motion, and arrest. Finally we identify combinations of parameters (surface length scales, particle size, flow rates) where particles can be manipulated with size-selectivity.

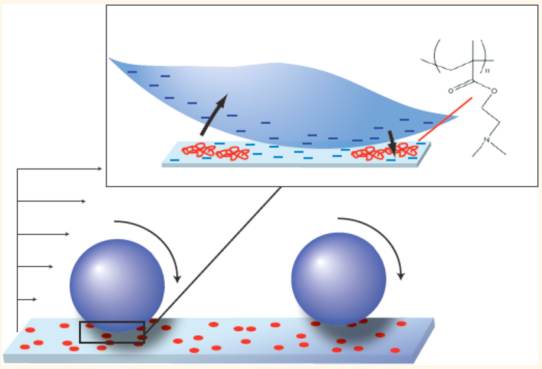

KEYWORDS: cell rolling · dynamic adhesion · leukocyte · neutrophil · hydrodynamics · selective particle capture · particle sorting · motion signature · microfluidics · microcapsules · renewable surfaces · self-cleaning surfaces · polyelectrolyte · surface charge · electrostatic

The shape of a microfluidic flow channel and its surface derivatization are key to microfluidic functions, from the mixing of streams to electrokinetic transport. Interactions of suspended particles or cells with the channel wall can facilitate selective capture, sorting, and detection. Growing research focusing on reactive microcapsules[1−5] sparks our interest in new microfluidic operations such as selective contact-mediated transfer of reagents or signals between a wall and microcarriers. While some microfluidic detectors may simply require arrest of targeted particles on an active surface region, more sophisticated online devices will be made possible by microfluidic surfaces over which particles or cells roll continuously to maintain an actively renewing surface for long exposure periods. Rolling is a powerful motion signature because intimate contact is achieved between a particle and the wall and because the contact times are well-defined, offering control over chemical reactions and signaling.

An understanding of microparticle rolling has emerged from studies of flowing white blood cells that roll within the vasculature (part of the immune response)[6,7] and from microsphere models of cell rolling.[8−10] Cell rolling is also relevant to the capture and manipulation of rare circulating tumor cells and other cell sorting operations[11−14] and to the harvesting of stem cells from blood.[15,16] In these instances, collecting surfaces are functionalized with cell adhesion molecules such as selectins or antibodies against cell markers.[17−20] Current understanding of cell capture and rolling includes the highly specialized response of force-sensitive selectin bonds[21,22] and their dynamic coupling with hydrodynamics and cell mechanics.[22,23] The complex interplay of many different variables necessitated the computational development of multidimensional state-space maps to describe

* Address correspondence to santore@mail.pse.umass.edu.

Received for review September 19, 2014 and accepted March 10, 2015.

Published online March 16, 2015
10.1021/nn505322m

the interfacial cell motion.[24,25] Beyond the focus on immobilized biomolecular fragments to manipulate cells[11,14,16] and particles,[21,26] the design of microfluidic channels for sustained particle rolling is in its infancy.

We expect the next advances in microfluidic manipulation of particles and cells will involve entirely synthetic functionalization of flow channel walls, engineered for precise dynamic interactions with flowing particles, microcapsules, and cells. Toward this vision, we incorporate discrete adhesive surface features on fundamentally nonadhesive or repulsive surfaces rather than developing uniform surface chemistries, a strategy inspired by discrete bonds in the cell rolling paradigm. Further, our use of relatively flat nanoscale features that interact *via* physical forces (van der Waals and electrostatics) contrasts with the classical tribological approach, where surface roughness imparts static and rolling friction that varies with normal force, usually from gravity.[27−29] Gravitational forces on suspended microparticles are often small and normal forces can vanish, depending on the orientation of the wall (relative to gravity) and on the density of particles relative to the fluid. When gravity cannot be relied upon to produce the normal forces and rolling friction, physicochemical interactions could prove a more reliable and more versatile approach.

We previously identified one surface design that facilitated the rolling of 1 μm diameter microspheres captured on surfaces in shearing flow.[30] That work focused on demonstrating that rolling was, in fact, occurring. The collecting surface was a negatively charged glass substrate containing randomly distributed isolated cationic polymer chains, pDMAEMA (polydimethylaminoethyl methacrylate) configured as flatted random coils with diameters of ~10 nm and average spacings on the order of tens of nanometers. The background negative surface charge was an important component of the design, necessary to overcome substantial van der Waals forces that would have overwhelmed the impact of the attractive surface features. The pDMAEMA chains, each comprising an attractive surface feature, were effectively irreversibly anchored to the substrate by strong physisorption.[31,32] Because of their low surface loadings, the cationic pDMAEMA chains had negligible influence on the overall negative charge of the wall;[33] however, the cationic pDMAEMA coils were individually weakly attractive toward flowing negative microparticles, acting as electrostatically adhesive "nanopatches" that could bond reversibly to flowing negative particles.[34] The weakly attractive character of individual adsorbed pDMAEMA "patches" toward approaching microparticles was important in that the interaction of particles with several patches at once was a requirement for particle adhesion.

The current work focuses on design strategies that incorporate nanoscale surface functionality to direct near-surface particle motion and, in particular, rolling. Focusing on a typical choice for a single type of electrostatically adhesive nanoscopic feature, the current study compares different interfacial particle behaviors (free flow, rolling, arrest) near a series of negatively charged surfaces having different densities of these nanoscopic features. The adhesive features are single coils of cationic pDMAEMA on silica, illustrated schematically in Figure 1. The current study also examines systematic variations in the ranges of the attractions and repulsions, flow rates, and particle sizes. The combined influence of these different material and engineering process parameters is developed into state space maps that highlight the confluence of materials and processing parameters when rolling occurs. The current study also examines how rolling velocities and run lengths depend on these materials and system features.

Aside from the direct significance of this work in guiding nanoscale surface designs for microfluidic manipulations of particles, the work is important in its description of surface features derived from a synthetic nanoscale object (here a synthetic homopolymer coil), instead of biomolecular fragments or adhesion molecules such as selectins, typically employed in the manipulation of cell rolling.[14−16,35] Synthetic homopolymers, such as the cationic acrylic in this work, are more economical than biomolecular fragments and may also be more robust, for instance, increasing ease of handling or shelf life. While we focus here on one cationic feature type and on a particular negative surface (glass), these choices are relevant to applications and fall in the middle of materials parameter space. Then with these materials choices, broad variations in other surface and processing parameters demonstrate the broad range of dynamic particle behaviors. This work demonstrates the use of these synthetic interfacial features to produce rolling in rigid nonbiological particles, but we envision extension to soft synthetic microcapsules and, ultimately, cells. Beyond microfluidic applications and platforms for particle-based diagnostics or for fundamental studies in biology, the fundamental understanding of dynamic microparticle adhesion afforded by this study may also facilitate regenerative surfaces,[36,37] improved surface polishing and cleaning methods,[38−40] new drug delivery schemes,[41,42] and improved understanding of particulate contaminants in soils.[43,44]

RESULTS

Suspensions of silica microspheres were flowed through a laminar slit chamber, and the dynamics of hundreds to thousands of near-surface particles were studied by video-microscopy in each run. Suspensions were relatively dilute with a microparticle concentration of 0.1 wt %, a level where the concentration did not influence particle−surface interactions or other

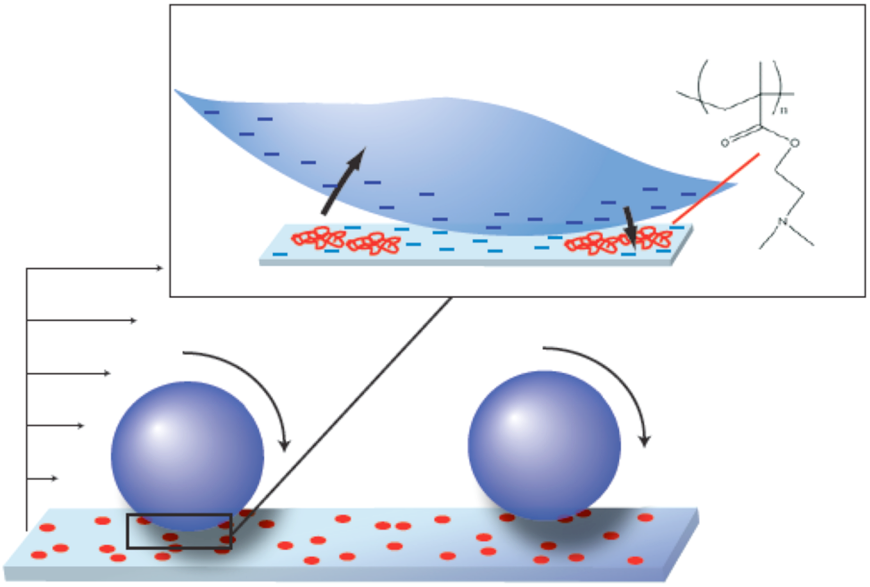

Figure 1. System schematic: 1 μm silica spheres, with a negative surface charge, flow over a negative silica surface containing sparsely and randomly positioned cationic polymer coils that localize positive charge and are attractive toward the silica sphere. Bare silica substrate areas repel the approach of silica microspheres. When rolling in shear flow, the electrostatic interactions at the leading edge form an effective bond that is disrupted in the rear of the particle as it rolls by.

findings. Further, a custom video-microscope oriented the test surface perpendicular to the floor to avoid gravitational contributions to normal particle–surface forces. (Also, gravity-driven particle settling parallel to the surface but normal to the flow direction adds negligibly to the torque from the pressure-driven shear flow.) The test surfaces themselves were silica, onto which different small amounts of the cationic polymer pDMAMEA were bound by strong physisorption, as shown in Figure 1. Prior studies revealed substantial cationic charge associated with sparsely adsorbed pDMAEMA coils but a negative charge on other regions of the silica surface.[33] The pDMAEMA is adsorbed flat to the surface[45] in a random distribution and is not removed and does not diffuse laterally during extended buffer flow[31,32] or exposure to flowing particles.[46] In the current work, pDMAEMA coils comprise isolated nanoscale surface features that localize cationic charge.

Three Behaviors: Rolling, Arrest, and Free Flow. Examples of particle positions and velocities for these three behaviors are shown in Figure 2, for typical 1 μm diameter microspheres tracked over surfaces of different compositions: arrest on a surface of relatively uniform cationic charge, rolling on a surface with nanoscale cationic features, and free flow past a surface of relatively uniform negative charge (bare silica). Apparent in these near-surface particle trajectories are qualitative differences in the appearance of arrest, rolling, and free flow. The rolling particle exhibits the smallest nonzero velocity. Both interesting and typical, when a freely flowing particle adheres statically or "arrests firmly" on a surface of uniform opposite charge, it undergoes a capture process involving rapid and immediate arrest without first slowing or rolling on the surface. Any gradual deceleration is not apparent at 30 frames/s.

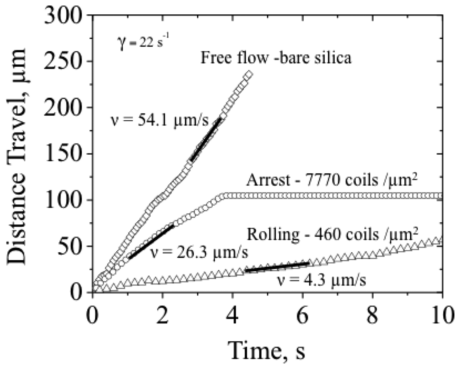

Figure 2. Typical single-particle trajectories on three different surfaces, exhibiting different motion signatures. The wall shear rate is γ = 22 s^{-1}, and the Debye length is κ^{-1} = 2 nm. The three different surfaces are indicated: bare silica, silica with 460 pDMAEMA coils/μm^2, and silica with 7700 pDMAEMA coils/μm^2.

Rolling particles are distinguished from freely flowing particles close to the wall by their translational velocities. For a known particle radius, a, and wall shear rate, γ, there exists a velocity, V_{crit}, below which the particle must be engaged with the wall (through friction or transient chemical bonds) and above which it must be freely flowing along a near-surface streamline. This occurs because when a particle flows freely, its translational velocity V exceeds the product of its radius and angular rotation rate, Ω. V_{crit} is calculated from the solution to the equations of motion developed by Goldman *et al.*[47] For 1 μm diameter particles flowing at a wall shear rate, γ, of 22 s^{-1} in Figure 2, V_{crit} = 5.3 μm/s.

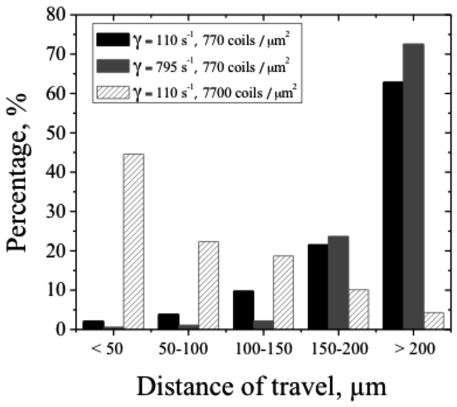

Figure 3. Distances traveled by particles moving more slowly than V_{crit} for different conditions: 288 particles at γ = 110 s^{-1} and 770 coils/μm^2; 139 particles at γ = 110 s^{-1} and 7700 coils/μm^2; 186 particles at γ = 795 s^{-1} and 770 coils/μm^2. The Debye length is κ^{-1} = 2 nm.

Distance of Travel. The velocity-based criterion for rolling identifies when an individual particle is undergoing a rolling motion. We are interested in describing, more generally, when surface designs facilitate rolling of targeted flowing particles. Rolling is, in general, deterministic, depending on the probability of a particle encountering an adhesive region and the probability of a surface−particle bond breaking within a given time window.[13,48] In identifying whether a surface is one on which targeted particles tend to roll (for a given set of flow and processing conditions), it is useful to impose an additional criterion concerning the length of travel during rolling: Different particles may roll for different lengths on a surface, and when particles roll into and out of the field of view, quantifying the rolling distance can be difficult. A particle that rolls only for a distance equal to a few of its diameters (and then arrests or diffuses away) is not undergoing a useful type of rolling for purposes of microfluidic manipulation. We therefore chose a cutoff for the required length of travel to distinguish surfaces that "facilitate particle rolling". We chose a travel distance of 50 particle diameters, somewhat arbitrarily, but in a fashion where the identification of surfaces as "supporting" or "not supporting" rolling is insensitive to the exact cutoff. We note that this criterion is consistent with, but more rigorous than, the minimum rolling distance of ∼5 particle diameters that is sometimes imposed within the cell rolling community.[14]

Figure 3 illustrates typical distributions of rolling travel distances for 1 μm silica spheres flowing in a buffer having a 2 nm Debye length near a surface with an adhesive pDMAMEA feature density of 770 /μm^2. This behavior is compared with flow near more adhesive surfaces containing 7700 pDMAEMA coils/μm^2. One always finds particles that, at some instants, are moving sufficiently slowly to be considered rolling, and all such particles are included in Figure 3. For the densely functionalized surface, however, these slow particles travel only for short distances before arresting. On the nanopatterned surface, however, rolling occurs for protracted distances, often beyond the 240 μm field of view. Applying the criterion of a 50-diameter rolling travel distance therefore turns out to be simple in practice, since large numbers of particles roll the maximum that is visible. Additionally in Figure 3, the fraction of particles traveling long distances increases slightly with flow rate.

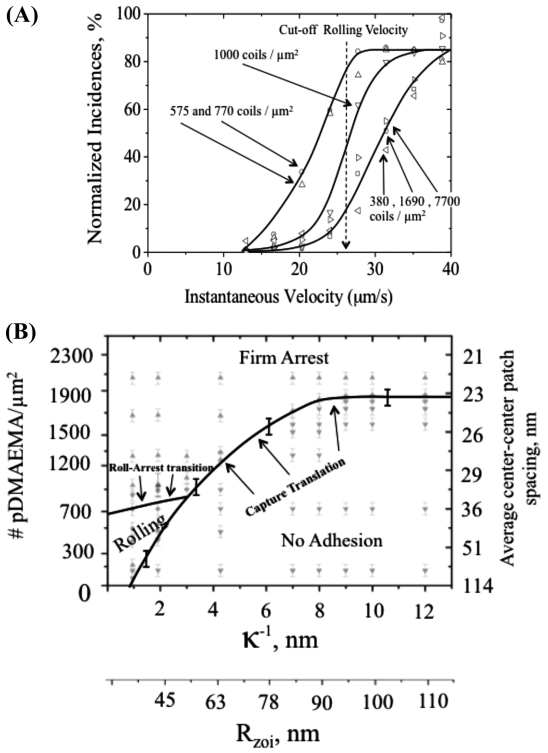

Figure 4. (A) Distribution of instantaneous particle velocities on different surfaces, for 1 μm diameter spheres, κ^{-1} = 2 nm, γ = 110 s^{-1}. (B) State space diagram for 1 μm silica spheres, γ = 110 s^{-1}.

Dependence of Rolling on Surface Design. Figure 4A summarizes the velocities of near-surface, 1 μm diameter microspheres in suspensions flowing at a wall shear rate of γ = 110 s^{-1} past surfaces with different densities of cationic polymer coils. These populations were the slowest moving particles (and therefore the ones nearest the surface) observed in the 14.2 s time window, a limitation set by our image analysis program. In each 14.2 s analysis period, between 1000 and 10 000 velocity measurements (all that were possible) were made for all the particles in the near-wall region of focus. Differences in the concentration boundary layers near the different surfaces were expected and controlled the number of moving near-surface particles. Also, more particles were studied (but for shorter periods of time) in runs with faster flow. Only moving particles were counted in Figure 4, as arrested particles accumulated in growing numbers on the more adhesive surfaces. Worth mentioning, the focusing optics on the microscope imaged the particles touching the

surface and those slightly off the surface as well, so some free particles were always included in the data and are distinguished by their faster velocities.

In Figure 4A, on surfaces having polycation loadings of 575 and 770 PDMAEMA coils/μm^2, corresponding to average coil spacings of 42 and 36 nm, a large fraction of near-surface particles traveled at velocities consistent with rolling. Not surprising, particles flowing over less adhesive surfaces such as silica functionalized with minute amounts of cationic features (for instance 380 pDMAEMA coils/μm^2, with an average spacing exceeding 51 nm) tended to translate at the free stream velocities and were not engaged with the surface. Fascinating, however, is the observation that similarly rapid translational velocities, corresponding to free particle flow, were also observed on strongly adhesive surfaces, with more than 1690 pDMAEMA coils/μm^2 (with an average spacing of 24 nm or less). The fast translation past strongly adhesive surfaces is explained in Figure 2, where the particle arrests abruptly after rapid free translation.

For the example case in Figure 4 with a wall shear rate of 110 s^{-1} and a Debye length of 2 nm, surfaces that enabled rolling of 1 μm particles were found to have spatial distributions of adhesive functionality and surface length scales in the range 30−45 nm. Surfaces with average feature spacings outside this window did not support rolling at these flow rates and ionic strengths. By comparison, on more densely cationic surfaces (containing polycationic loadings greater than 1690 pDMAMEA coils/μm^2 or average feature spacings less than 24 nm), silica particles arrested immediately, as shown in Figure 2. The free particle velocities before arrest, however, were similar to those seen on the nonadhesive bare silica surface. Apparent in Figure 4A is the relatively sharp distinction between surfaces on which particles exhibit rolling *versus* arrest or free flow: Intermediate behavior, for a loading of 1000 polycation coils/μm^2, is distinct and lies at the boundary between rolling and arrest.

Data from Figure 4A, along with additional measurements made at different ionic strengths and different surface loadings, are summarized in Figure 4B, all for a wall shear rate of γ = 110 s^{-1}. This representation is termed a "variable state space map". The *x*-axis of Figure 4B is the Debye length. The *y*-axis describes the surface loading of adhesive cationic polymer coils. In the context of these parameters, particle behavior is described as nonadhesive, dynamically adhesive (rolling), or firmly adhesive (arrest). The error bars correspond to a few percent surface loading of pDMAEMA coils and represent the uncertainty both in surface fabrication and in applying the rolling criteria discussed in the context of Figures 3 and 4A. This type of state space map, following the concept of the neutrophil rolling literature,[24,25] describes behavior for a single type of adhesive element and background

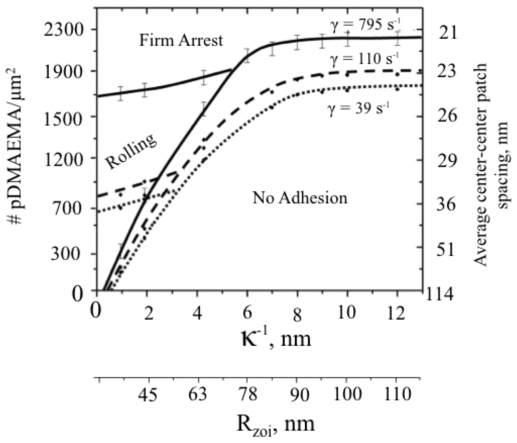

Figure 5. Superposed state spaces for 1 μm particles at γ = 39, 110, and 795 s^{-1}.

surface composition, along with fixed choices for particle size and flow rates. Additional maps would be needed to describe the impact of these additional parameters.

In addressing the question of when rolling of 1 μm silica spheres is sustained, Figure 4B demonstrates that surface design is not the sole consideration. Consider in Figure 4B a vertical path, for instance at a fixed Debye length of 5 or 6 nm, traversing particle behaviors on a series of surfaces of increased loading of cationic adhesive features. As the surface is made stickier in this way, the system moves from a regime where microparticles flow freely to one where they arrest quickly without rolling as they flow past and diffuse toward the surface. For relatively large Debye lengths or longer ranges in the surface forces, no matter how adhesive (or not) the surface, particles are not observed to undergo rolling. Striking, however, is the observation that rolling becomes a possibility for appropriately designed surfaces, as long as the Debye length, describing the range of both attractions and repulsions, is sufficiently small.

Effect of Flow. For 1 μm silica spheres, Figure 5 superposes several variable state space diagrams for wall shear rates of γ = 39, 110, and 795 s^{-1}. In combining three variable state space maps into a single diagram, the same surface compositions and ionic strengths were tested for each state space map (at each flow rate/particle size combination) as exemplified by the multitude of points in Figure 4B; however, the data points themselves could not be drawn in Figure 5 because of the different boundaries for the different velocities and transitions. Figure 5 therefore focuses on the boundaries between the different regimes of particle behavior and how these transitions in dynamic behavior shift with flow rate. Error bars on the boundaries reflect a 2% uncertainty in the loadings of polycation coils.

Figure 5 quantifies how shear makes particle adhesion more dynamic: The size of the nonadhesive region

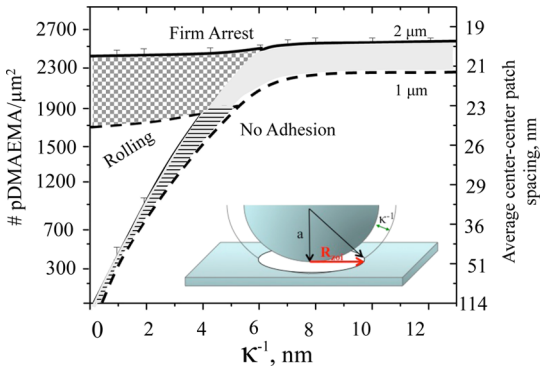

Figure 6. Superposed state spaces for 1 and 2 μm particles with γ = 795 s^{-1}. Area shaded gray is where small particles adhere but big ones do not. Checkered area where big particles roll but small arrest. Striped area is where small particles roll, but big ones are rejected.

of the state space is increased with increased wall shear, quantifying how adhesion is opposed by hydrodynamic force. At large Debye lengths the surface functionality needed for particle capture from flow increases weakly with flow. Flow dramatically increases the variable space that enables particle rolling.

Effect of Particle Size. Figure 6 superposes state diagrams for two different monodisperse particle sizes, 1 and 2 μm, flowing past surfaces with a wall shear rate of 795 s^{-1}. These two sizes were chosen, rather than a pair with greater size differences, to address the resolution in separating or discriminating the dynamic behavior of closely sized particles. At the same time, comparison of 1 and 2 μm particles reveals the quantitative impact of particle diameter: larger particles tend to be less adhesive than smaller ones. One reason is that, with the hydrodynamic shear force on a particle scaling as the particle radius squared, greater attractions are needed to retain large particles on a surface. Figure 6 also quantifies how large particles generally roll more readily than small ones, with a greater portion of the variable space supporting rolling of large particles.

Of great potential for microfluidic operations are the three shaded regions highlighted in Figure 6. Here near-surface particle behavior is dynamically selective. For example, at Debye lengths exceeding about 5 nm, there exist surface compositions containing about 2200−2400 polycationic coils/μm^2 that selectively capture and arrest 1 μm particles, while the 2 μm particles flow freely past. At Debye lengths smaller than about 5 nm and surface compositions between 1200 and 2400 polycation coils/μm^2, the hatched shaded area is a region of state space where 1 μm particles adhere firmly but 2 μm particles roll over the surface. Finally, the narrow region shaded with stripes indicates a combined range of Debye lengths (below about 5 nm) and corresponding polycation loadings, below 1700 coils /μm^2, where 1 μm particles roll along the surface, but 2 μm particles are nonadhesive. Worth noting, the variable state space map anticipates these selective behaviors based on studies of suspensions containing single particle types. While studies with mixtures would be needed to confirm these predictions, we expect them to hold to the extent that the state space represents the behavior of individual particles in dilute suspension, without particle−particle interactions. Indeed our prior work has shown a rigorous translation of single-particle behavior to that in dilute mixtures,[49] along with the ability to access narrow windows of selective behavior with modest efforts to fabricate surfaces with precision.[50]

The influence of particle size on the boundaries in state space parallels the influence of flow rate because hydrodynamic forces scale as the square of the particle size. Hydrodynamic forces influence both the ability of particles to roll (as oppose to arrest) and to be captured in the first place. The particle diameter also comes into play through the effective particle−surface interaction area,[49] illustrated in the inset of Figure 6. More gradually curved (larger) particles interact with a greater area of the wall, with the radius, R_{zoi}, of this interactive "zone" scaling as the square root of the particle radius, a, and Debye length, κ^{-1}. The impact of the different effective contact on attractions and repulsions is discussed below. Implicit in this definition of R_{zoi} is that the attractive and repulsive electrostatic forces have the same range, which is the case for our surfaces, since the attractions and repuslsions are both electrostatic in nature. It is clear, however, that the large contact areas involving larger flowing particles ensure that the particle experiences the more average character of the wall, in these cases net electrostatically negative and repulsive to negative particles. Smaller flowing particles interact with smaller regions of the wall and are more susceptible to the fluctuations of attractions and repulsions. While the radius of the interactive zone is included as a second x-axis in Figures 4B and 5, it could not be included in Figure 6 because the two particle sizes experience different interactive zones. Also, replacing the Debye length with R_{zoi} failed to collapse the state space maps for the two particle sizes to a master map.

DISCUSSION

This work demonstrates a strategy to engineer surfaces that facilitate rolling of flowing spherical microparticles and it identifies conditions, for the particular class of surfaces, where such rolling can and cannot occur. Inspired by the concept of discrete ligand−receptor bonds responsible for cell capture and rolling in blood, the work focuses on surfaces that electrostatically attract microparticles *via* discrete nanoscale features. Equally important is the negative charge on the rest of the surface, providing a background repulsive field that must be overcome by the adhesive surface elements in capturing the particles.

Without the background repulsion, van der Waals forces would dominate adhesion, masking any impact of the cationic adhesive nanofeatures. It also turns out to be important to the quantitative results here that the discrete electrostatic attractions and the background repulsion are in the same range, the Debye length. (One might imagine other repulsive mechanisms, for instance steric repulsion, which would be decoupled from the length scales of the attractive features. Such a system might begin to be understood from the current work.) Thus, variations in the Debye length, on the *x*-axis of the state spaces of Figures 4B, 5, and 6, produce the same increases in the zone of influence, R_{zoi}, for the interactive area applicable to both attractions and repulsions. Further, it is important that the adhesive surface features are randomly distributed on the surface. Because the individual pDMAEMA–microparticle interactions are weak, several immobilized pDMAMEA coils must interact with a microparticle to facilitate its capture. The probability of this happening depends on the random distribution of the pDMAEMA coils and on the size of the interactive zone. Particles are captured on regions of the surface having greater than average local densities of adhesive features.[34]

While this study employed a single type of adhesive element, the capture behavior of silica microspheres (summarized in the state space as the boundary between free flow and either type of adhesion) is consistent, except for quantitative details, with prior reports of capture on surfaces containing immobilized cationic nanoparticles[50] or a molecular weight range of pDMAMEA chains of 16 000–100 000 g/mol.[51] While we did not quantify rolling in those other studies, we believe that the current state spaces qualitatively describe behavior that could be found in other related systems and that the current report is not a unique case.

An important take-home message from this study is that, while nanoscopic surface features can be designed and arranged to ensure the rolling of particles captured from a flowing suspension, the choice of surface parameters must take into account system features such as particle size, flow rate, and the range of both attractions and repulsions, for instance *via* the ionic strength. Surfaces that enable particle rolling are not "one-size-fits-all". Further, it is not possible to identify a single scaling relationship involving fundamental variables such as particle size and flow rate, because the different physical mechanisms acting on flowing particles scale differently with these system variables. (Hydrodynamic forces scale as a^2, van der Waals forces scale as a, and electrostatic interactions have a more complicated dependence on particle size, depending on the Debye length.) Other length scales such as the zone of influence, which collapses the Debye length and particle size into a physically meaningful term, still cannot provide a single simple relationship for predicting rolling. For this reason the variable state space approach works well to help conceptualize the regimes of different particle behavior in terms of the different length scales.

A corollary to the message about the utility of variable states' space and the choice of surface variables is that conditions exist, for instance at large Debye lengths, where it seems not possible to achieve particle rolling with any member of the surface library in this study. It is fascinating that, as one increases particle–surface adhesion strength by titrating more adhesive features onto the surface, the transition from free flow to particle arrest occurs abruptly with no rolling window. At small Debye lengths, however, increased particle–surface adhesion is manifest by two transitions, one from flow to dynamic rolling adhesion and a second from rolling to arrest. The Debye length affects particle–surface interactions in complex ways in these systems with heterogeneous walls. Not only does it control the range of attractive and repulsive electrostatic particle–surface interactions, it also affects the area of the wall exerting force on the particle in a fashion similar to particle size, and it affects the apparent heterogeneity of the wall: cationic patches, situated closer than a Debye length to each other, cannot be distinguished by an approaching object. (In the current study, however, the electrostatic isolation of the cationic patches is generally met throughout the variable state space.)

The state space boundary between free flow and arrest or rolling, as a function of Debye length, is determined by the probability of a flowing particle being captured into a rolling or arrested state. Such capture requires that the flowing particle encounter, locally, a sufficient number of adhesive coils in the zone of influence (exceeding the average number of pDMAEMA coils/area) to overcome hydrodynamic interactions and the background electrostatic repulsion. If the attractive and repulsive potentials grow similarly with Debye length, one might estimate that a fixed local number of adhesive elements per unit area would be needed for capture, independent of Debye length, as was confirmed for similar systems.[34] However, as the R_{zoi} is increased *via* the Debye length, the repulsion per particle grows as R_{zoi}^2. The attraction per particle grows less slowly with increases in R_{zoi} (*via* the Debye length) as a result of the random distribution of the attractive elements: It becomes more difficult to locate such a critical "hot spot" in the distribution of adhesive elements when the interaction area is larger. The resulting increase in the capture boundary of state space with Debye length follows: the surface must be more densely loaded with adhesive features to capture microspheres. Without distinguishing between rolling or arrested particle fate, we previously established that a Poisson distribution for the arrangement of adhesive patches on a repulsive surface adequately

predicted the surface compositions for the onset of particle capture.[34]

The fates of captured particles (rolling or arrest) is determined by a second boundary in state space and is most sensitive to flow than to other parameters studied: Increased flow pushes particles over the surface and provides rotational motion (torque), key to rolling. A more subtle distinction, however, between parameters that support rolling as opposed to arrest comes from the distribution of local adhesive elements relative to other length scales. When a particle rolls, "bonds" in the rear of the particle are broken and new ones in front must quickly form, maintaining sufficient numbers to keep the particle captured. With sufficient hydrodynamic force to break the bonds in the rear of the particle, the surface in front of the particle must present sufficient probability for the particle to find new "bonds". In the limit of small Debye lengths and small R_{zoi}'s, only a few such bonds need to form as the particle moves forward. Larger numbers of bonds are needed at larger Debye lengths and larger zones of influence.[34] The probability of finding an adequate number of interactive groups to meet the requirements at large Debye lengths may be smaller unless the surface is loaded more densely to begin with. In this case, however, the particle may be held too firmly to move forward. These ideas concerning the interplay of surface and hydrodynamic forces along with the statistical probability of bond formation are being developed in ongoing work.

The findings reported here are significant in both their fundamental implications and their technological potential: The current work demonstrates design rules for sustained rolling in an entirely synthetic (nonbiological) system including the particles themselves. This contrasts with the role of specialized adhesion molecules in directing cell rolling and the rolling of particle models for cells. Potentially of great technological power is that the current model system exhibits sustained rolling under the control of *electrostatic* forces, which are a fairly ubiquitous type of interaction in aqueous suspensions and microfluidics. It is the tight nanoscale manipulation of the in-plane and surface-normal nanoscale length scales of these forces that is the key to achieving rolling. Further, in achieving rolling for a broad range of flow rates (and hydrodynamic forces), we have not targeted an interfacial design with a force-sensitive disbonding rate. By contrast, the force sensitivity of the disbonding rate of the selectins is an important feature of the cell rolling mechanism.[7,22,25]

This work has demonstrated how clustering and spatial modulation of electrostatic charge can facilitate rolling of negative spherical particles. It remains an open question the extent to which the variable state spaces presented here can be applied to other related systems, for instance cells or bacteria that are not perfectly spherical, that are deformable to varying extents, and that present, in addition to negative surface charge, other surface chemistries and inherent length scales for these surface chemistries (contrasting the uniform negative character of our model silica microspheres). It may be possible that related variable state spaces could result by simply shifting the boundaries on the current state space or that an addition dimension to the state space would need to account for the mechanical properties of soft spherical objects.

A final thought concerning rolling of microparticles is worth emphasizing. Rolling is a common every day behavior seen with macroscopic objects including car wheels, toy balls, and rocks on a hillside, and so it is easy to assume that rolling is also a preferred type of interfacial motion for microparticles in flow near a surface. With this (incorrect) intuition, the results of the current study would seem of negligible significance, in that one would expect microparticles to roll on just about any surface, as long as adhesion is not too strong or too weak. The state spaces of Figures 4B, 5, and 6 refute this intuition for microparticle behavior, at the same time explaining why rolling is more common for large particles: Bigger particles experience larger windows of variable space that support rolling. Conversely, the combinations of variables that support rolling for small microparticles are quite limited and become increasingly small as one extrapolates the state space diagrams to smaller length scales. While the literature contains accounts of the "rolling" of nanoscale objects (micelles or proteins for instance),[52−54] the behavior may not constitute true rolling: Vorticity will cause an object to rotate, but dynamic adhesion must be appropriately tuned for that rotation to produce rolling travel along a surface. Indeed direct evidence for an actual rolling motion or appropriate near-surface velocity is rarely provided in the case of micelles. Smaller objects require greater shear fields in order to experience rolling because small objects span more nearly similar streamlines at an interface and therefore will be less likely to experience sufficient torque to overcome Brownian forces.

CONCLUSIONS

This study examined the use of weakly adhesive nanoscale features, placed randomly on the electrostatically repulsive wall, to facilitate rolling of negatively charged microparticles in shear flow. The use of relatively flat nanoscopic features to produce forces critical to particle rolling in the absence of substantial gravitational normal forces contrasts with classical systems in the field of tribology (including studies of roughness and rolling friction). Likewise, the use of a synthetic homopolymer as the adhesive surface element contrasts with the surface immobilization of selectins and other biomolecules exhibiting complex functionality.

Microparticle rolling was identified and quantified in a series of systems dominated by electrostatic

interactions. The motion of near-surface particles was characterized and velocities and near-surface travel distances were measured for negative microspheres of two sizes. Many variables were systematically studied: the surface loadings of adhesive nanoscale features, the range of attractive and repulsive interactions, and variations in flow. It was found that, in order to sustain particle rolling, surface designs needed to account not only for the nature of the particles themselves but also for the flow and the ionic strength. There was no simple rule of thumb or design equation that could predict rolling and collapse all the relevant system variables. It was, however, enlightening to describe the behavior of particle motion in a multivariable state space, which delineated the combinations of variables producing particle rolling, firm arrest, and free flow.

For a particular choice of particle and flow rate, if rolling were to be supported, it required surfaces with small amounts of adhesive nanoscale features. The Debye length, which set the range of particle−surface interactions, was critical in establishing whether rolling could be sustained. While rolling could proceed on appropriately designed surfaces (for targeted particles and a given flow rate) at small Debye lengths, rolling did not occur when the Debye length was large, regardless of the surface design. At large Debye lengths, as particle−surface adhesion was made increasingly attractive by the incorporation of increased amounts of adhesive nanoscale functionality on the collecting surface, particle behavior transitioned directly from free flow to firmly arrested adhesion. By contrast at small Debye lengths, as adhesion to the collecting surface was potentially strengthened by increasing the adhesive feature density, the particle motion transitioned from free flow, to rolling, and finally to arrest. The result argues for a complex interplay of dynamic length scales, forces, and time scales in determining particle rolling. Without a large literature on the control of particle rolling and arrest *via* discrete chemical surface features, we are cautioned in generalizing these results. However, we note that negatively charged surfaces, such as those in the current system, abound in microfluidic devices and the electrostatic repulsion was a key component in our surface design. Also potentially important in defining the regimes where our observations apply, with flat electrostatically attractive features on an otherwise electrostatically repulsive surface, variations in Debye length changed the ranges of the attractions and repulsions together and to the same extent. Interfaces with different physicochemical origins for the attractions and repulsions (*e.g.*, one electrostatic and the other steric) would experience different relative variations in the ranges of the attractions and repulsions and might behave somewhat differently than the surface designs presented here.

It was additionally demonstrated that for variable combinations producing rolling, the rolling travel length was may times the particle diameter and increased with flow rate. A sensitivity of rolling to particle size was also demonstrated, and regions of state space were identified where targeted particles could be made to roll selectively.

MATERIALS AND METHODS

The 1 μm silica microspheres were purchased from GelTech (Orlando, FL, USA) and used as received. The 2 μm silica microspheres were purchased from Bang's Laboratories and used as received. Both were tightly monodisperse. The relatively similar sizes allowed us to probe the potential selectivity of our surfaces. While a wide range in sizes might ultimately be desired to address the full size range in a physical study, limits are set by the Stober process and by our ability to track particle velocities at the low magnifications needed to also track long particle trajectories. While submicrometer particles are regularly imaged optically these days, a large travel field requires low magnification, which is at odds for visualizing submicrometer particles.

Engineered surfaces were made by adsorbing pDMAEMA on microscope slides that had been soaked in concentrated sulfuric acid overnight to produce a silica surface. The pDMAEMA, 31 300 in molecular weight and with a polydispersity near 1.2, was a gift from DuPont. It was transferred from its original THF solution to an aqueous solution by rotary evaporation. The absence of THF was confirmed by ^{1}H NMR spectroscopy.

pDMAEMA deposition and subsequent silica particle adhesion from flow were studied sequentially in the same slit-shear flow chamber (1 cm × 3 cm × 0.5 mm) without removal of the substrate or exposing it to air. Targeted amounts of pDMAEMA were deposited from flowing pH 6.1 phosphate-buffered solution, having an ionic strength of 0.026 M and a Debye length of 2 nm. This buffer was made from 0.0234 M KH_2PO_4, with an extremely small amount of 0.000267 M NaOH added, if needed, to adjust the pH. After buffer flow over the surface at 5 s^{-1}, the solution was switched to 20 ppm pDMAEMA for varied amounts of time, on the order of a few seconds or a few minutes, and then switched back to buffer to halt the adsorption at the desired point. Buffer continued to flow for 10 min. In the current study, the pDMAEMA adsorption was not monitored *in situ*. Its adsorption rate and retention on the surface had, however, been previously studied exhaustively *via* optical reflectometry, such that controlled amounts could be deposited within 2% error by timed flow.[34,46] These reproducible adsorption curves, measured by reflectometry, provide a calibration curve for the timed deposition in the current work. Following the polymer adsorption step, any necessary changes in buffer ionic strength or flow rate were made, and the system was allowed to reach steady state at the new conditions. Subsequently, particle flow experiments commenced. The ionic strength or Debye length was set by using different buffers. For instance, the stock buffer (I = 0.026 M, used during pDMAEMA adsorption) was diluted in DI water, to produce buffers with large Debye lengths. A pH 6.1 buffer with a 1 nm Debye length was made using 0.0936 M KH_2PO_4 and adjusting the pH with a very small amount of dilute NaOH.

Silica microparticle flow and adhesion employed 0.1 wt % suspensions of 1 or 2 μm diameter microspheres. The flow chamber was mounted in a custom-built lateral microscope with the substrate perpendicular to the floor. The microscope configuration employed a 10× Nikon phase contrast objective, illumination from behind, and a video camera, which recorded

images at the standard rate of 30 s^{-1}. Data stored on DVD were subsequently analyzed using ImageJ and IDL software. This provided counts of particles in each frame and allowed the identities of particles in one frame to be correlated with those in the next frame so that instantaneous velocities could be determined. Each particle position and the velocity of each particle between each frame in a stack of 200 frames (the limit of the software) were recorded in a spreadsheet.

The analysis programs yielded several perspectives on the capture of flowing particles on these surfaces. One type of direct result was a count of the increasing number of particles on a surface as a function of time. A second level of analysis tracked particle motion, allowing a determination of whether or not each particle was engaged with the surface. Regarding the accumulation of microparticles as a function of time, this study focused on relatively short times within each run, where the surface was sufficiently empty of captured particles such that those already on the surface did not alter the capture rate or surface behavior of new particles.[30] This led to a linearity in the number of captured particles as a function of time, a feature that persisted well beyond the first 10 min of each run. Also, control studies of particle rolling involved analyzing different 200-frame stacks of data, comparing behaviors taken shortly after the initiation of a run with those several minutes, up to 10, into the run. Particle accumulation of the "rolling surfaces" was minimal. Particle accumulation on the "arrest surfaces" was substantial but, because of the precautions taken, did not influence the reported measurements.

Polymer adsorption studies of pDMAEMA on silica revealed features of the interface relevant to this particle rolling study. Of primary importance, the adsorbed pDMAEMA was not removed in buffer or particle flow at any of the conditions in this study,[31,32,46] nor could we detect lateral diffusion of the polymer or exchange between adsorbed chains with those free in solution during separate challenge studies at conditions like those discussed here. Also worth noting, the pDMAEMA coils were individually shown to be adsorbed flat to the surface[45] and are thought to have a random coil configuration with a diameter less than 10 nm, based on dynamic light scattering studies of the solution. Saturated adsorbed layers of pDMAEMA (approximately 0.4 mg/m^2on silica) exhibited substantially positive zeta potentials depending on ionic strength, indicating that the individual coils were positively charged at the interface.[33] At the surface loadings in the current study, however, the adsorbed amount of pDMAEMA is relatively low so that the zeta potentials were all net negative.[46] Indeed the small amounts of adsorbed pDMAEMA needed to produce rolling did not substantially alter the overall negative surface charge on the collecting surface. Finally, the average spacings between adsorbed pDMAEMA coils result from knowledge of the adsorbed pDMAEMA mass and molecular weight. The mass per area is converted (*via* molecular weight) to numbers of coils per area, and this term is inverted to give the area per coil. The square root is the average center−center spacing between the coils.

Conflict of Interest: The authors declare no competing financial interest.

Acknowledgment. This work was supported by NSF 12-64844.

REFERENCES AND NOTES

1. Alexeev, A.; Verberg, R.; Balazs, A. C. Patterned Surfaces Segregate Compliant Microcapsules. *Langmuir* **2007**, *23*, 983–987.
2. Fery, A.; Dubreuil, F.; Mohwald, H. Mechanics of Artificial Microcapsules. *New J. Phys.* **2004**, *6*, 18.
3. MacDonald, M. P.; Neale, S.; Paterson, L.; Richies, A.; Dholakia, K.; Spalding, G. C. Cell Cytometry with a Light Touch: Sorting Microscopic Matter with an Optical Lattice. *J. Biol. Regul. Homeostatic Agents* **2004**, *18*, 200–205.
4. Nie, Z. H.; Xu, S. Q.; Seo, M.; Lewis, P. C.; Kumacheva, E. Polymer Particles with Various Shapes and Morphologies Produced in Continuous Microfluidic Reactors. *J. Am. Chem. Soc.* **2005**, *127*, 8058–8063.
5. Shum, H. C.; Kim, J.-W.; Weitz, D. A. Microfluidic Fabrication of Monodisperse Biocompatible and Biodegradable Polymersomes with Controlled Permeability. *J. Am. Chem. Soc.* **2008**, *130*, 9543–9549.
6. Janeway, C. A.; Travers, P.; Walport, M.; Shlomsik, M. J. *Immunobiology: The Immune System in Health and Disease*, 6th ed.; Garland Science Publishing: New York, 2005.
7. Lawrence, M. B.; Springer, T. A. Leukocytes Roll on a Selectin at Physiological Flow-Rates - Distinction from and Prerequisite for Adhesion through Integrins. *Cell* **1991**, *65*, 859–873.
8. Brunk, D. K.; Goetz, D. J.; Hammer, D. A. Sialyl Lewis(X)/E-Selectin-Mediate Rolling in a Cell-Free System. *Biophys. J.* **1996**, *71*, 2902–2907.
9. Brunk, D. K.; Hammer, D. A. Quantifying Rolling Adhesion with a Cell-Free Assay: E-Selectin and Its Carbohydrate Ligands. *Biophys. J.* **1997**, *72*, 2820–2833.
10. Eniola, A. O.; Willcox, P. J.; Hammer, D. A. Interplay between Rolling and Firm Adhesion Elucidated with a Cell-Free System Engineered with Two Distinct Receptor-Ligand Pairs. *Biophys. J.* **2003**, *85*, 2720–2731.
11. Edington, C.; Murata, H.; Koepsel, R.; Andersen, J.; Eom, S.; Kanade, T.; Balazs, A. C.; Kolmakov, G.; Kline, C.; McKeel, D.; Liron, Z.; Russell, A. J. Tailoring the Trajectory of Cell Rolling with Cytotactic Surfaces. *Langmuir* **2011**, *27*, 15345–15351.
12. Nagrath, S.; Sequist, L. V.; Maheswaran, S.; Bell, D. W.; Irimia, D.; Ulkus, L.; Smith, M. R.; Kwak, E. L.; Digumarthy, S.; Muzikansky, A.; Ryan, P.; Balis, U. J.; Tompkins, R. G.; Haber, D. A.; Toner, M. Isolation of Rare Circulating Tumour Cells in Cancer Patients by Microchip Technology. *Nature* **2007**, *450*, 1235–U10.
13. Choi, S. Y.; Karp, J. M.; Karnik, R. Cell Sorting by Deterministic Cell Rolling. *Lab Chip* **2012**, *12*, 1427–1430.
14. Lee, C. H.; Bose, S.; Van Vliet, K. J.; Karp, J. M.; Karnik, R. Examining the Lateral Displacement of Hl60 Cells Rolling on Asymmetric P-Selectin Patterns. *Langmuir* **2011**, *27*, 240–249.
15. Hughes, A. D.; Mattison, J.; Western, L. T.; Powderly, J. D.; Greene, B. T.; King, M. R. Microtube Device for Selectin-Mediated Capture of Viable Circulating Tumor Cells from Blood. *Clin. Chem.* **2012**, *58*, 846–853.
16. Wojciechowski, J. C.; Narasipura, S. D.; Charles, N.; Mickelsen, D.; Rana, K.; Blair, M. L.; King, M. R. Capture and Enrichment of Cd34-Positive Haematopoietic Stem and Progenitor Cells from Blood Circulation Using P-Selectin in an Implantable Device. *Br. J. Hamaetol.* **2008**, *140*, 673–681.
17. Adams, A. A.; Okagbare, P. I.; Feng, J.; Hupert, M. L.; Patterson, D.; Gottert, J.; McCarley, R. L.; Nikitopoulos, D.; Murphy, M. C.; Soper, S. A. Highly Efficient Circulating Tumor Cell Isolation from Whole Blood and Label-Free Enumeration Using Polymer-Based Microfluidics with an Integrated Conductivity Sensor. *J. Am. Chem. Soc.* **2008**, *130*, 8633–8641.
18. Becker, C.; Pohla, H.; Frankenberger, B.; Schuler, T.; Assenmacher, M.; Schendel, D. J.; Blankenstein, T. Adoptive Tumor Therapy with T Lymphocytes Enriched through an Ifn-Gamma Capture Assay. *Nat. Med.* **2001**, *7*, 1159–1162.
19. Hong, S.; Lee, D.; Zhang, H.; Zhang, J. Q.; Resvick, J. N.; Khademhosseini, A.; King, M. R.; Langer, R.; Karp, J. M. Covalent Immobilization of P-Selectin Enhances Cell Rolling. *Langmuir* **2007**, *23*, 12261–12268.
20. Karnik, R.; Hong, S.; Zhang, H.; Mei, Y.; Anderson, D. G.; Karp, J. M.; Langer, R. Nanomechanical Control of Cell Rolling in Two Dimensions through Surface Patterning of Receptors. *Nano Lett.* **2008**, *8*, 1153–1158.
21. Greenberg, A. W.; Brunk, D. K.; Hammer, D. A. Cell-Free Rolling Mediated by L-Selectin and Sialyl Lewis(X) Reveals the Shear Threshold Effect. *Biophys. J.* **2000**, *79*, 2391–2402.
22. Hammer, D. A.; Apte, S. M. Simulation of Cell Rolling and Adhesion on Surfaces in Shear-Flow - General Results and Analysis of Selectin-Mediated Neutrophil Adhesion. *Biophys. J.* **1992**, *63*, 35–57.

23. Chang, K. C.; Hammer, D. A. The Forward Rate of Binding of Surface-Tethered Reactants: Effect of Relative Motion between Two Surfaces. *Biophys. J.* **1999**, *76*, 1280–1292.
24. Bhatia, S. K.; King, M. R.; Hammer, D. A. The State Diagram for Cell Adhesion Mediated by Two Receptors. *Biophys. J.* **2003**, *84*, 2671–2690.
25. Chang, K. C.; Tees, D. F. J.; Hammer, D. A. The State Diagram for Cell Adhesion under Flow: Leukocyte Rolling and Firm Adhesion. *Proc. Natl. Acad. Sci. U.S.A.* **2000**, *97*, 11262–11267.
26. Zhang, Y.; Milam, V. T.; Graves, D. J.; Hammer, D. A. Differential Adhesion of Microspheres Mediated by DNA Hybridization I: Experiment. *Biophys. J.* **2006**, *90*, 4128–4136.
27. Bardet, J. P. Observations on the Effects of Particle Rotations on the Failure of Idealized Granular-Materials. *Mech. Mater.* **1994**, *18*, 159–182.
28. Smart, J. R.; Beimfohr, S.; Leighton, D. T. Measurement of the Translational and Rotational Velocities of a Noncolloidal Sphere Rolling Down an Smooth Inclined Plane at Low Reynolds Number. *Phys. Fluids A* **1993**, *5*, 13–24.
29. Krijt, S.; Dominik, C.; Tielens, A. G. G. M. Rolling Friction of Adhesive Microspheres. *J. Phys. D: Appl. Phys.* **2014**, *47*, 175302.
30. Kalasin, S.; Santore, M. M. Sustained Rolling of Microparticles in Shear Flow over an Electrostatically-Patchy Surface. *Langmuir* **2010**, *26*, 2317–2324.
31. Hansupalak, N.; Santore, M. M. Sharp Polyelectrolyte Adsorption Cutoff Induced by a Monovalent Salt. *Langmuir* **2003**, *19*, 7423–7426.
32. Hansupalak, N.; Santore, M. M. Polyelectrolyte Desorption and Exchange Dynamics near the Sharp Adsorption Transition: Weakly Charged Chains. *Macromolecules* **2004**, *37*, 1621–1629.
33. Shin, Y. W.; Roberts, J. E.; Santore, M. M. The Relationship between Polymer/Substrate Charge Density and Charge Overcompensation by Adsorbed Polyelectrolyte Layers. *J. Colloid Interface Sci.* **2002**, *247*, 220–230.
34. Duffadar, R.; Kalasin, S.; Davis, J. M.; Santore, M. M. The Impact of Nanoscale Chemical Features on Micron-Scale Adhesion: Crossover from Heterogeneity-Dominated to Mean-Field Behavior. *J. Colloid Interface Sci.* **2009**, *337*, 396–407.
35. Cheung, L. S.-L.; Zheng, X.; Wang, L.; Baygents, J. C.; Guzman, R.; Schroeder, J. A.; Heimark, R. L.; Zohar, Y. Adhesion Dynamics of Circulating Tumor Cells under Shear Flow in a Bio-Functionalized Microchannel. *J. Micromech. Microeng.* **2011**, *21*, 54033–54042.
36. Wisdom, K. M.; Watson, J. A.; Qu, X.; Liu, F.; Watson, G. S.; Chen, C.-H. Self-Cleaning of Superhydrophobic Surfaces by Self-Propelled Jumping Condensate. *Proc. Natl. Acad. Sci. U.S.A.* **2013**, *110*, 7992–7997.
37. Kolmakov, G. V.; Revanur, R.; Tangirala, R.; Emrick, T.; Russell, T. P.; Crosby, A. J.; Balazs, A. C. Using Nanoparticle-Filled Microcapsules for Site-Specific Healing of Damaged Substrates: Creating a "Repair-and-Go" System. *ACS Nano* **2010**, *4*, 1115–1123.
38. Goldasteh, I.; Ahmadi, G.; Ferro, A. R. Monte Carlo Simulation of Micron Size Spherical Particle Removal and Resuspension from Substrate under Fluid Flows. *J. Aerosol Sci.* **2013**, *66*, 62–71.
39. Gradon, L. Resuspension of Particles from Surfaces: Technological, Environmental and Pharmaceutical Aspects. *Adv. Powder Technol.* **2009**, *20*, 17–28.
40. Mercier-Bonin, M.; Adoue, M.; Zanna, S.; Marcus, P.; Combes, D.; Schmitz, P. Evaluation of Adhesion Force between Functionalized Microbeads and Protein-Coated Stainless Steel Using Shear-Flow-Induced Detachment. *J. Colloid Interface Sci.* **2009**, *338*, 73–81.
41. Cui, Y.; SchmalfuSs, S.; Zellnitz, S.; Sommerfeld, M.; Urbanetz, N. Towards the Optimisation and Adaptation of Dry Powder Inhalers. *Int. J. Pharm.* **2014**, *470*, 120–32.
42. Calderon, A. J.; Muzykantov, V.; Muro, S.; Eckmann, D. M. Flow Dynamics, Binding and Detachment of Spherical Carriers Targeted to Icam-1 on Endothelial Cells. *Biorheology* **2009**, *46*, 323–341.
43. Li, S.; Marshall, J. S.; Liu, G.; Yao, Q. Adhesive Particulate Flow: The Discrete-Element Method and Its Application in Energy and Environmental Engineering. *Prog. Energy Combust. Sci.* **2011**, *37*, 633–668.
44. Lazouskaya, V.; Wang, L.-P.; Or, D.; Wang, G.; Caplan, J. L.; Jin, Y. Colloid Mobilization by Fluid Displacement Fronts in Channels. *J. Colloid Interface Sci.* **2013**, *406*, 44–50.
45. Shin, Y.; Roberts, J. E.; Santore, M. M. Influence of Charge Density and Coverage on Bound Fraction for a Weakly Cationic Polyelectrolyte Adsorbing onto Silica. *Macromolecules* **2002**, *35*, 4090–4095.
46. Kozlova, N.; Santore, M. M. Manipulation of Micrometer-Scale Adhesion by Tuning Nanometer-Scale Surface Features. *Langmuir* **2006**, *22*, 1135–1142.
47. Goldman, A. J.; Cox, R. G.; Brenner, H. Slow Viscous Motion of a Sphere Parallel to a Plane Wall 0.2. Couette Flow. *Chem. Eng. Sci.* **1967**, *22*, 653.
48. Alon, R.; Hammer, D. A.; Springer, T. A. Lifetime of the P-Selectin-Carbohydrate Bond and Its Response to Tensile Force in Hydrodynamic Flow. *Nature* **1995**, *374*, 539–542.
49. Santore, M. M.; Kozlova, N. Micrometer Scale Adhesion on Nanometer-Scale Patchy Surfaces: Adhesion Rates, Adhesion Thresholds, and Curvature-Based Selectivity. *Langmuir* **2007**, *23*, 4782–4791.
50. Santore, M. M.; Zhang, J.; Srivastava, S.; Rotello, V. M. Beyond Molecular Recognition: Using a Repulsive Field to Tune Interfacial Valency and Binding Specificity between Adhesive Surfaces. *Langmuir* **2009**, *25*, 84–96.
51. Kalasin, S.; Martwiset, S.; Coughlin, E. B.; Santore, M. M. Particle Capture *via* Discrete Binding Elements: Systematic Variations in Binding Energy for Randomly Distributed Nanoscale Surface Features. *Langmuir* **2010**, *26*, 16865–16870.
52. Arya, G.; Panagiotopoulos, A. Z. Log-Rolling Micelles in Sheared Amphiphilic Thin Films. *Phys. Rev. Lett.* **2005**, *95*, 188301.
53. Kratz, K.; Narasimhan, A.; Tangirala, R.; Moon, S.; Revanur, R.; Kundu, S.; Kim, H. S.; Crosby, A. J.; Russell, T. P.; Emrick, T.; Kolmakov, G.; Balazs, A. C. Probing and Repairing Damaged Surfaces with Nanoparticle-Containing Microcapsules. *Nat. Nanotechnol.* **2012**, *7*, 87–90.
54. Peng, B.; Chu, X.; Li, Y. Y.; Li, D. S.; Chen, Y. M.; Zhao, J. Adsorption Kinetics and Stability of Poly(Ethylene Oxide)-Block-Polystyrene Micelles on Polystyrene Surface. *Polymer* **2013**, *54*, 5779–5789.